
Nonlinear Moment Reversal Behavior in Steel Frames

Ali Abolmaali¹, Member, ASCE, AISC, and SSRC
Yeol Choi², Member, AISC and ACI

INTRODUCTION AND BACKGROUND

In conventional frame analysis, connections between beams and columns are ordinarily treated as either perfectly rigid or pinned. Perfectly rigid connections (moment connections) allow full transfer of moment from beam to column. Pinned connections are commonly referred to as shear connections which act as hinges and allow full transfer of shear and axial forces between beam and column, but they do not allow transfer of moment. In reality, beam-to-column connections are neither fully rigid nor perfectly flexible and are known as semi-rigid connections. The behavior of semi-rigid connections is quantified by their moment-rotation relationship the shape and degree of nonlinearity of which depend on connection's geometric and material variables. This nonlinearity is attributed to number of factors such as material discontinuity of the connection assemblage, local yielding of connection components, stress concentration at bolt holes and fasteners, geometric changes under applied loads, and local plate buckling (Chen et al. 1996).

The moment rotation behavior (M- θ) of steel connections is commonly obtained by experimental testing. Several researchers have reported static M- θ test data of connections among these studies Chen et al. (1996) and Chen and Lui (1991) are known for their comprehensive M- θ data base. Also, several cyclic M- θ connection behavior known as hysteresis behavior are reported in literature among which Popov and Bertero (1973), Tsai et al. (1995), Astaneh et al. (1989), Kukreti and Abolmaali (1999), and Abolmaali et al. (2003) are referenced in this paper.

The realization of the effect of semi-rigid joints on overall frame behavior can be traced back to 1930s. Baker (1931) and Rathbun (1936) first applied conventional slope deflection and moment distribution to semi-rigid frame analysis, respectively. Monforton and Wu (1963) were first to incorporate the effect of flexible joints into matrix stiffness method. This was done by modifying beam-column element stiffness matrix to incorporate the effect of semi-rigidity. Similar algorithms were also introduced by Livesley (1964) and Gere and Weaver (1965). In these algorithms a linear moment-rotation connection curve and a factor were used to modify the beam-column element stiffness matrix. The dynamic behavior of frames with flexible joints was studied by Lionberger and Gere (1969) and Suko and Adams (1971) in which semi-rigid connections

¹ Assistant Professor of Structural Engineering and Mechanics
Structural Simulation Laboratory
University of Texas at Arlington, Arlington, Texas 76019
E-mail: abolmaali@ce.uta.edu

² Post Doctoral Research Scientist
Structural Simulation Laboratory
University of Texas at Arlington, Arlington, Texas 76019
E-mail: choi@ce.uta.edu

were modeled by elasto-plastic rotational springs. Lightfoot and LeMessurier (1974) conducted investigations on semi-rigid frame analysis considering axial and shear deformations. From 1974 to 1991 more than twenty matrix stiffness method-based semi-rigid frame analysis techniques are reported among which Nethercot (1986); Goto and Chen (1987); Lui and Chen (1987); Poggi (1988); and Goto et al (1991) are mentioned here. Li et al (1995) presented a connection element method, which allows for joint flexibility associated with all the required degrees-of-freedom for beam column element, including coupling between deformations. King and Chen (1993) proposed a practical LRFD-based analysis method for analysis of frames with semi-rigid connections in which a simplified three-parameter model describing the tangential rotational stiffness of the semi-rigid connections was presented. Bhatti and Hingegen (1995) examined the effect of certain parameters on serviceability limit-state of unbraced frames. Rodrigues et al (1998) introduced a fictitious connection element with finite and infinite stiffness for its rotational and translational degrees of freedom, respectively. During the same time Christopher and Bjorhovde (1998) investigated semi-rigid frame stability by using an effective beam stiffness that is modified for moment-rotation behavior of the connection to determine unbraced column length factor. Finally, Kukreti and Abolmaali (2000) presented a nonlinear finite element algorithm for analysis of semi-rigid frames subjected to earthquake ground acceleration.

Most of the aforementioned studies and those not referenced in this paper do not specifically address the effect of connection unloading on frame stability due to connection moment redistribution at different incremental load levels. In semi-rigid frames subjected to distributed loads, connections' stiffness decays with increasing moment. At bifurcation, some connections unload as the result of buckling due to rotation reversal Chen et al (1996). During unloading, the stiffness of each unloaded connection increases and equals to the initial stiffness, which consequently increases the frame stiffness and enables it to withstand additional load beyond bifurcation. On the other hand, if column of a frame is subjected to concentrated load in absence of the member loads, none of the connections will unload until bifurcation. Upon bifurcation the connection's stiffness decreases and no unloading will take place, and frame becomes unstable. Also, frames made of different types of connections with different moment-rotation characteristics, could undergo unloading in certain connections depending on beam and column's flexural rigidities.

The aforementioned discussion shows the complex and unknown behavior of semi-rigid frames, which necessitates a detailed analysis technique that considers connection unloading. Indeed, during unloading some connection may undergo reverse loading the effect of which needs to be incorporated in the analysis.

ANALYSIS ALGORITHM WITH CONNECTION UNLOADING

This paper presents a plasticity-based solution method that iterates to find the simultaneous incremental member and geometric stiffness of the structure subjected to loading of its members, and loading, unloading, and reverse loading of its connections. Based on finite element procedures, a steel frame with flexible joints can be considered as an assembly of beam-column elements and dimensionless rotational spring elements. Linear displacement based finite element, yields to the solution of linear equations:

$$[k]\{\delta\} = \{F\} \quad (1)$$

Where $\{F\}$ is the force vector containing all loads applied to the degrees of freedom of the structure, $[K]$ is the global stiffness matrix, and $\{\delta\}$ is the global displacement matrix. The stiffness of a beam-column element (including P- δ effect) in global coordinate is:

$$[k] = [k_{ea}] + [k_{eb}] + [k_g] \quad (2)$$

where $[k_{ea}]$ is the element axial stiffness matrix, $[k_{eb}]$ is the element bending stiffness matrix, and $[k_g]$ is the geometric stiffness matrix. The matrices of Equation 2 is defined in most matrix structural analysis text books such as Gere and Weaver (1965).

The connections were modeled as dimensionless spring elements with the same translational but different rotational degrees of freedom (DOF) to model the relative rotation of the beam and column end rotations as shown in Figure 1. The relative rotation of the spring element is calculated as follows:

$$\theta_r = \theta_1 - \theta_2 \quad (3)$$

where θ_1 and θ_2 are the beam-end and column-end rotations, respectively. Rotational degrees of freedom between beam and column are governed by the spring stiffness. The behavior of the spring is quantified only by the relationship between applied moment and relative rotation. The spring tangent stiffness matrix is formulated to be compatible with the classical beam-column element by making it a matrix of 6x6 in size, and its non-zero elements are: $k_{33}=k_{66}=k$ and $k_{36}=k_{63}=-k$.

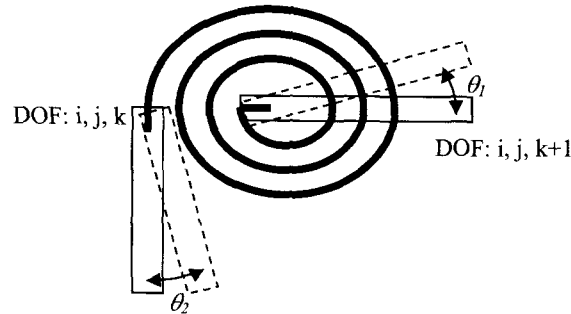


Figure 1 Connection Element

The spring stiffness, K (Equation 6), is defined as the derivative of the kinematic hardening equation (Equation 4), with respect to relative rotation θ_r :

$$M = R_{ki} \theta_r \left(\frac{1 - R_b / R_{ki}}{\{1 + [(1 - R_b / R_{ki}) \theta_r / \theta_o]^n\}^{1/n}} + \frac{R_b}{R_{ki}} \right) \quad (4)$$

where; R_{ki} is the initial connection stiffness, R_b = slope of the asymptotic line, n is a shape parameter, and θ_0 = reference plastic rotation given by:

$$\theta_0 = \frac{M_u}{R_{ki}} \quad (5)$$

where M_u is the ultimate connection moment. The tangent stiffness of the connection for any value of rotation is given by:

$$K = \frac{dM}{d\theta_r} = AD + ABE^{(-1/n)} - ABC^n \theta_r^n E^{(n-1-2/n)} \quad (6)$$

where

$$A = R_{ki} \quad (7)$$

$$B = 1 - R_b/R_{ki} \quad (8)$$

$$C = B/\theta_0 \quad (9)$$

$$D = R_b/R_{ki} \quad (10)$$

$$E = 1 + C^n \theta_r^n \quad (11)$$

NONLINEAR SOLUTION METHOD

This study employs direct iteration method to solve the nonlinear system equation. The direct iteration method was used as an alternative to the classical Newton-Raphson method. In this method, the first load increment is solved using the initial stiffness, and in the subsequent load steps the stiffness of the connection is updated as follows:

$$k_{i+1} = \xi k_i + (1 - \xi) k_{is} \quad (12)$$

where

- k_{i+1} = stiffness for the next load increment
- ξ = descent parameter
- k_i = stiffness from the previous load increment
- k_{is} = secant stiffness from the previous load increment

The secant stiffness is calculated by finding the actual moment for the calculated rotation from the previous iteration solution. The descent parameter can be any number between 0 and 1, which if taken as 0 implies that next iteration stiffness yields to secant stiffness. In certain

instances using a higher descent parameter can result in a more stable solution path. In direct iteration method, instead of applying an unbalanced load to the structure to achieve convergence, a weighted effective stiffness is sought to satisfy the nonlinear system equation. For the first iteration in a given load increment, the tangent stiffness is used. Thus, using the linear approximation of the first iteration, member displacements and forces are calculated and used to provide a better approximation of the effective stiffness across the incremental load step. For the connection element, the updated connection stiffness is found by calculating current iteration cycle secant modulus and obtaining a weighted average between it and the tangent modulus of previous iteration. The actual connection moment for a given relative rotation is obtained by using Equation 4 and dividing it by the relative rotation to find the secant stiffness in each iteration cycle.

For the beam-column, the stiffness for the next iteration cycle is obtained by substituting the geometric stiffness matrix from the elastic stiffness matrix using the axial force found for each member in the current iteration cycle. This is relatively simple for the first increment of load. For subsequent load steps, however, incremental stiffness is not as simple to calculate. Figure 2 represents the conceptual solution path for a single beam-column element, which is split up into two load increments. The first incremental solution is shown between the origin and point A. For the first load increment, a load of $\{f_1\}$ is applied to the element and the element undergoes a displacement $\{d_1\}$. The equation to be solved in the first load increment is:

$$\{f_1\} = \left([k_e] - [k_{g1}] \right) \{d_1\} \quad (13)$$

where $\{f_1\}_{6 \times 1}$ is the member force matrix for the first load increment, $[k_e]_{6 \times 6}$ is the sum of the axial and bending element stiffness matrices, $[k_{g1}]_{6 \times 6}$ is the geometric stiffness matrix for the first load increment (a function of axial force), and $\{d_1\}_{6 \times 1}$ is the displacement matrix for the element for the first increment of load. Similarly, for the second incremental set of member forces $\{f_2\}$, the equation that applies to the situation is

$$\{f_1\} + \{f_2\} = \left([k_e] - [k_{g2}] \right) (\{d_1\} + \{d_2\}) \quad (14)$$

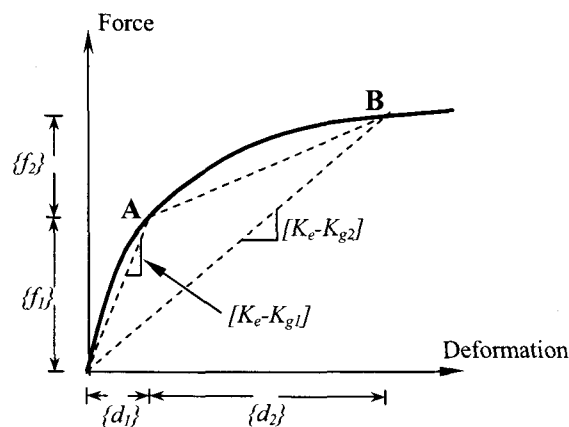


Figure 2 Conceptual Representation of Incremental Solution

Where $\{f_2\}_{6 \times 1}$ is the incremental member force matrix for the second increment of load, $[k_{g2}]_{6 \times 6}$ is the geometric stiffness matrix for the total load after the second increment (a function of total axial load), and $\{d_2\}_{6 \times 1}$ is the incremental displacement matrix for the second load increment. The previous equation reveals the problem of trying to apply the geometric stiffness matrix to an incremental solution method. It applies only to the total solution and not to the second increment of force alone. In order to apply an incremental solution, an equation of the following form is needed in order to apply the direct iteration method in terms of the second second set of incremental member forces:

$$\{f_2\} = [k_{effective}] \{d_2\} \quad (15)$$

To begin the process of putting together an equation of the form of Equation 13, Equations 10 and 11 can be rearranged as follows:

$$\{f_2\} = [k_e] \{d_2\} + [k_{g1}] \{d_1\} - [k_{g2}] \{d_1\} - [k_{g2}] \{d_2\} \quad (16)$$

The problem that becomes evident in Equation 14 is that there is no apparent way to isolate the right side of the equation in terms of the second incremental displacement $\{d_2\}$. However, Equation 16 can be further manipulated as follows:

$$\{f_2\} = ([k_e] + ([k_{g1}] - [k_{g2}]) \{d_1\} \{\alpha\} - [k_{g2}]) \{d_2\} \quad (17)$$

where $\{\alpha\}$ can be defined as a 1x6 matrix subject to two conditons:

$$\{\alpha\} \{d_2\} = [1] \text{ (a 1x1 matrix)} \quad (18)$$

$$([k_{g1}] - [k_{g2}]) \{d_1\} \{\alpha\} = \text{a square 6x6 symmetric matrix} \quad (19)$$

The constraint in Equation (18) is insufficient alone to solve for $\{\alpha\}$ because there are infinite number of solutions to that equation. The symmetric constraint of Equation 19 brings the number of solutions for $\{\alpha\}$ to exactly one. The reason that the symmetric constraint is valid is because the member stiffness matrix must be symmetric or else the beam-column elements will not obey equilibrium. Subject to the given constraints, the $\{\alpha\}$ matrix is calculated as follows:

$$\alpha_6 = \frac{\phi_6}{\phi_1 d_{i(1)} + \phi_2 d_{i(2)} + \phi_3 d_{i(3)} + \phi_4 d_{i(4)} + \phi_5 d_{i(5)} + \phi_6 d_{i(6)}} \quad (20)$$

$$\alpha_5 = \frac{\phi_5 (1 - \alpha_6 d_{i(6)})}{\phi_1 d_{i(1)} + \phi_2 d_{i(2)} + \phi_3 d_{i(3)} + \phi_4 d_{i(4)} + \phi_5 d_{i(5)}} \quad (21)$$

$$\alpha_4 = \frac{\phi_4(1 - \alpha_6 d_{i(6)} - \alpha_5 d_{i(5)})}{\phi_1 d_{i(1)} + \phi_2 d_{i(2)} + \phi_3 d_{i(3)} + \phi_4 d_{i(4)}} \quad (22)$$

$$\alpha_3 = \frac{\phi_3(1 - \alpha_6 d_{i(6)} - \alpha_5 d_{i(5)} - \alpha_4 d_{i(4)})}{\phi_1 d_{i(1)} + \phi_2 d_{i(2)} + \phi_3 d_{i(3)}} \quad (23)$$

$$\alpha_2 = \frac{\phi_2(1 - \alpha_6 d_{i(6)} - \alpha_5 d_{i(5)} - \alpha_4 d_{i(4)} - \alpha_3 d_{i(3)})}{\phi_1 d_{i(1)} + \phi_2 d_{i(2)}} \quad (24)$$

$$\alpha_1 = \frac{(1 - \alpha_6 d_{i(6)} - \alpha_5 d_{i(5)} - \alpha_4 d_{i(4)} - \alpha_3 d_{i(3)} - \alpha_2 d_{i(2)})}{d_{i(1)}} \quad (25)$$

where

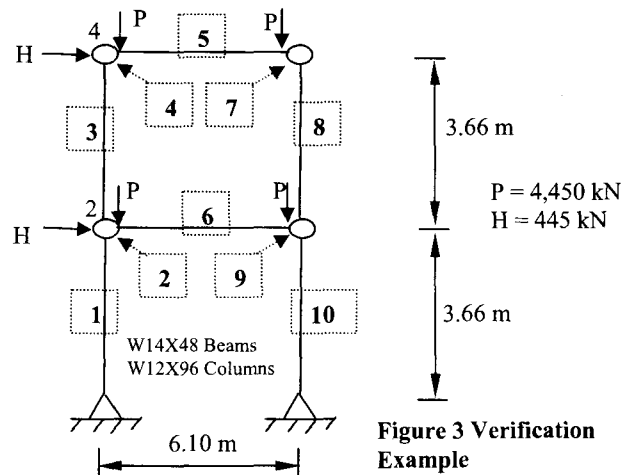
$$\{\phi\}_{6 \times 1} = \left(\left[k_{g2} \right] - \left[k_{g1} \right] \right) \{d_{i-1}\} \quad (26)$$

and $\{d_{i-1}\}_{6 \times 1}$ is the total displacement vector at the end of the previous load increment ($\{d_i\}$ (in the given example with two load increments)), and $\{d_i\}_{6 \times 1}$ is the member displacement matrix for the current load increment. With known $\{\alpha\}$, the effective stiffness for a given increment of load to be used in the direct iteration formulation is as follows:

$$\left[k_{effective} \right] = \left[k_e \right] + \left(\left[k_{g1} \right] - \left[k_{g2} \right] \right) \{d_i\} \{\alpha\} - \left[k_{g2} \right] \quad (27)$$

VERIFICATION

It was only possible to verify the aforementioned algorithm with those in literature without considering connection unloading. Thus, an example problem (as shown in Figure 3) was chosen from King and Chen (1993) and Bhatti and Hingtgen (1995) in which only the connection loading were considered in their semi-rigid frame analysis.



For the aforementioned examples no moment reversal was possible prior to column buckling due to the absence of loads on the beam. Using $R_{ki} = 88,892 \text{ KN-m/rad}$ (786732 k-in/rad), $R_b = 0$, $\theta_0 = 0.00252818 \text{ rad}$, and $n = 100$. Tables 1 and 2 present the comparison of the results of developed algorithm with those of aforementioned study reported in literature.

Table 1. Absolute maximum bending moments KN-m (k-in)

Element No.	Rigid Connections No P-Delta	Rigid Connections with P-Delta		Flexible Connections with P-Delta	
	Present Study	Present Study	Bhatti & Hingtgen	Present Study	Bhatti & Hingtgen
1	163 (1443)	189 (1677)	189 (1677)	196 (1739)	196 (1739)
3	80 (711)	90 (794)	90 (794)	102 (901)	102 (902)
5	80 (711)	90 (795)	90 (795)	102 (902)	102 (902)
6	163 (1450)	187 (1656)	187 (1654)	185 (1636)	185 (1634)
8	80 (711)	90 (795)	90 (795)	102 (902)	102 (902)
10	162 (1437)	189 (1669)	189 (1669)	196 (1732)	196 (1731)

Table 2. Lateral displacements m (in.)

Node No.	Rigid Connections No P-Delta	Rigid Connections with P-Delta		Flexible Connections with P-Delta	
	Present Study	Present Study	Bhatti & Hingtgen	Present Study	Bhatti & Hingtgen
2	0.02567 (1.011)	0.02966 (1.168)	0.02966 (1.168)	0.03752 (1.477)	0.03752 (1.477)
4	0.03883 (1.509)	0.04397 (1.731)	0.04397 (1.731)	0.0582 (2.292)	0.0582 (2.292)

EFFECTS OF CONNECTION UNLOADING

A parametric-type study was conducted on a simple one story-one bay frame with two connections, as shown in Figure 4, to identify the unloading behavior of one of the connection by varying the value of stiffness of the other connection. The connection on the left side and the one on the right side of the frame are designated as Connection 1 and Connection 2, respectively. The moment-rotation characteristics of each spring are assumed to be linear and elastic. To investigate the behavior of the frame, the stiffness of Connection 1 was held constant at the value of 11,299 kN-m/rad (100,000 kip-in/rad), and the stiffness of Connection 2 was varied between 0 and 22,599 kN-m/rad (200,000 kip-in/rad). Figure 5 shows the results of this analysis. As the stiffness of Connection 2 increases beyond 2,768 kN-m/rad (24,500 kip-in/rad), the sign of the moment across Connection 1 reverses. Thus, moment reversal in Connection 1 occurs as the value of Connection 2 stiffness drops below 2,768 kN-m/rad (24,500 kip-in/rad). This observation indicates that unloading can occur when a high degree of nonlinearity exists in the connections such that for a certain combinations of gravity and wind loads (or anti-symmetric loading) the stiffness of one connection would degrade more rapidly than stiffness of the other connection, and consequently causes unloading in the connection in which the degradation rate is slower. Moreover, if two different kinds of connections with different stiffness degradation rates (different $M-\theta$ curves) are used in the aforementioned frame, then, one of the connections will unload for the same applied moment.

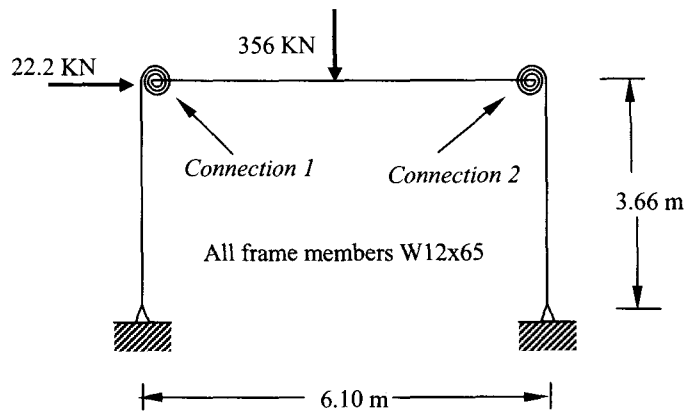


Figure 4 Frame Used to Investigate Connection Unloading Behavior

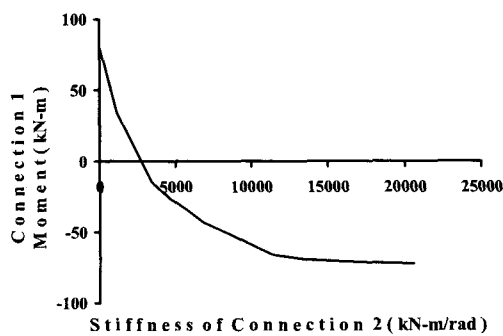


Figure 5 Effect of Connection 2 Stiffness on Connection 1 Moment

To further investigate the effect of stiffness of the Connection 2 on the sign of moment taken by Connection 1, the connections in frame of Figure 5 was modeled to represent a nonlinear $M-\theta$ behavior of a semi-rigid connection including kinematic hardening effects. The following values were used for the parameters of the kinematic hardening model of Equation 4 for connections of the frame in Figure 5:

Connection 1: $R_{ki} = 11,299 \text{ kN-m/rad}$ (100,000 k-in/rad), $R_b = 2,260 \text{ kN-m/rad}$ (20,000 k-in/rad), $\theta_o = 0.00005 \text{ rad}$, and $n = 50$.

Connection 2: $R_{ki} = 11,299 \text{ kN-m/rad}$ (100,000 k-in/rad), R_b varied between 2,260 kN-m/rad (20,000 kip-in/rad) and 3,390 kN-m/rad (30,000 k-in/rad), $\theta_o = 0.0002 \text{ rad}$, and $n = 50$.

Figure 6 shows the moment rotation models used for Connections 1 and 2 of the frame of Figure 5.

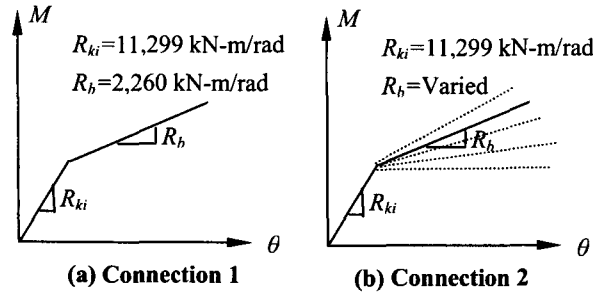
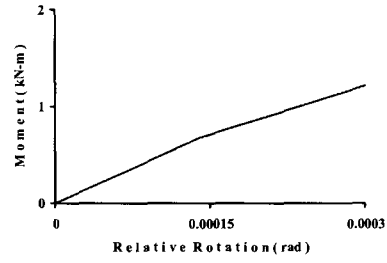


Figure 6 Moment Rotation Models

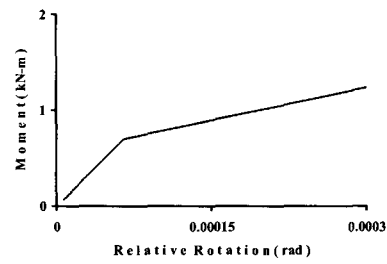
Figure 7(a) through 7(e) shows the history of variation of the moment in Connection 1 by varying the asymptotic stiffness, R_b , in Connection 2 for the same applied load. Figure 7 (a) indicates that for $R_b = 3,390$ kN-m/rad (30,000 k-in/rad) in Connection 2, Connection 1 behaves mostly linear. As asymptotic stiffness in Connection 2 is reduced to $R_b = 2,825$ kN-m/rad (25,000 kip-in/rad), Figure 7 (b) shows that Connection 1 continues to load in the same direction, but yields beyond its idealized elastic region. At $R_b = 2,768$ kN-m/rad (24,500 k-in/rad) for Connection 2, Connection 1 starts to unload as shown in Figure 7(c). Upon further reducing the values of asymptotic stiffness of Connection 2 to 2,757 kN-m/rad (24,400 kip-in/rad) and 2,260 kN-m/rad (20,000 kip-in/rad) as shown in Figures 7(d) and 7(e), respectively, Connection 1 continues to unload and yield in the unloading direction (Figure 7(e)). Thus, stiffness degradation of Connection 2 has caused Connection 1 to go through a complete unloading and reverse loading. This would cause redistribution of member forces, which is normally not taken into account in design procedures without considering joint unloading. Finally, Figure 7 (e) shows that moment rotation behavior of Connection 1 is of kinematic hardening types, which is the type implemented in the analysis algorithm.

CONCLUSIONS

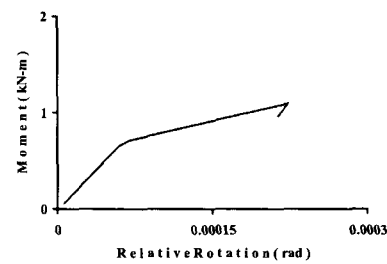
The effects of connection moment reversal (connection unloading) are commonly ignored in semi-rigid frame analysis, and increasing applied member load and/or joint moment is considered to degrade connection's stiffness. However, for connections connecting members with distributed loads or frames with different types of connections, unloading and reverse loading of connections are possible which causes connection stiffness to increase. This could result in redistribution of member forces, or in some cases, member bifurcation. Thus, a semi-rigid frame analysis algorithm is presented to investigate the unloading characteristics of semi-rigid connections under static proportional loading. A kinematic hardening equation to model the pseudo-cyclic behavior of semi-rigid connections is used. A unique and fast solution technique that simultaneously iterates to find the incremental connection element and member geometric stiffness of the structure is introduced to solve the nonlinear system equations. The proposed algorithm is used to investigate the effects of stiffness degradation of one semi-rigid connection on the moment reversal of the other connection in a simple frame.



(a)

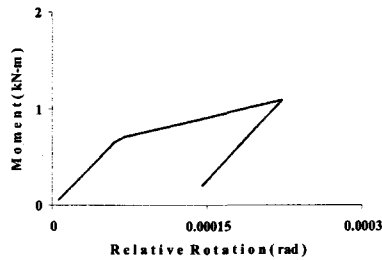


(b)

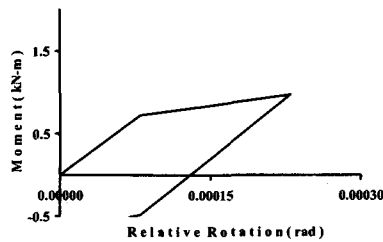


(c)

Figure 7 Moment Rotation Behavior of Connection 1 For Asymptotic Stiffness of Connection 2 : (a) 3,390 kN-m/rad; (b) 2,825 kN-m/rad; and (c) 2,760 kN-m/rad.



(d)



(e)

Figure 7 (continued) Moment Rotation Behavior of Connection 1 For Asymptotic Stiffness of Connection 2 : (d) 2,257 kN-m/rad and (e) 2,260 kN-m/rad

ACKNOWLEDGEMENT

The Financial support of the National Science Foundation (Grant # 0231404) is greatly acknowledged.

REFERENCES

1. American Institute of Steel Construction (1993). *Load and resistance factor design*, 2nd Edition.
2. Abolmaali, A., Kukreti, A. R., and Razavi, S. H., (2003), "Cyclic Performance of Semi-Rigid Double Web Angle Steel Connections." *Journal of Construction Steel Research*. No. 59, PP 1057-1082.
3. Astaneh, A., Nader, M.N., and Malik, L., (1989), "Cyclic Behavior of Double Web Angle Connections." *Journal of Structural Engineering*, ASCE, Vol. 115, No. 5, pp. 1101-1118.
4. Baker, J. P., *Methods of Stress Analysis*, First and Second Reports, Steel Structures Research Committee, HMSO, London, England, 1931 and 1934.
6. Bhatti, M.A., and Hingtgen, J.D. (1995) "Effects of connection stiffness and plasticity on the service load behavior of unbraced steel frames." *Engineering Journal*, AISC, Vol. 32, No.1, pp. 21-33.
7. Chen, W.F., Goto, Y., and Liew, R. (1996). *Stability design of semi-rigid frames*. John Wiley and Sons, New York.

-
8. Chen, W.F., and Lui, E.M. (1991). *Stability design of steel frames*. CRC Press, Boca Raton.
 9. Christopher, J. E. & Bjorhovde, R. Response characteristics of frames with semi-rigid connections, *Journal of Constructional Steel Research*, v 46, n 1-3, 1998, on CD ROM
 10. Gere, J. M., & Weaver, W., *Analysis of Frame Structures*. Van Nostrand, Princeton NJ, 1965.
 11. Goto, Y. & Chen, W. F., On the computer-based design analysis for the flexibly jointed frames. *Journal of Constructional Steel Research*, 8 (1987) 203-31.
 12. Goto, Y., Suzuki, S. & Chen, W. F., Analysis of critical behaviour of semi-rigid frames with or without load history in connections. *International Journal of Solids and Structures*, 27 (4) (1991) 467-83.
 13. King, W.S., and Chen, W.F. (1993). "LRFD Analysis for semi-rigid frame design." *Engineering Journal*, AISC, Vol. 30, No.4, pp. 130-140.
 14. Kukreti, A. R., and Abolmaali, A., (1999), "Moment-Rotation Hysteresis Behavior of Top and Seat Angle Steel Frame Connections." *Journal of Structural Engineering*, Vol. 125, No. 8, PP 810-820.
 15. Kukreti, A.R., and Abolmaali, A., (2000), "Dynamic Analysis of Steel Frames with Semi-Rigid Connections." *the XLXII Southeastern Conference on Theoretical and Applied Mechanics*, Deerfield Beach, Florida, May 13-16.
 16. Li, T. Q., Choo, B. S. & Nethercot, D. A., Connection element method for the analysis of semi-rigid frames, *Journal of Constructional Steel Research*, v 32, n 2, 1995, p 143-171
 17. Lightfoot, E. & Le Messurier, A. P., Elastic analysis of frameworks with elastic connections. *Journal of Structural Division, ASCE*, 89 (ST6) (June 1974) 1297-309.
 18. Lionberger, S. R. & Weaver, W., Jr, Dynamic response of frames with non-rigid connections. *Journal of the Engineering Mechanics Division, ASCE*, 95 (EMI) (February 1969) Proc Paper 6393, 95-114.
 19. Livesley, R. K., *Matrix Methods of Structural Analysis*, 1st edn. Pergamon Press, Oxford, 1964.
 20. Lui, E.M., and Chen, W.F. (1987). "Steel frame analysis with flexible joints." *Journal of Constructional Steel Research*, Vol. 8, pp. 161-202.
 21. Monforton, G. R. & Wu, T. S., Matrix analysis of semi-rigidly connected frames. *Journal of the Structural Division, ASCE*, 89 (ST 6) (December 1963) 13-42.
 22. Nethercot, D. A., The behaviour of steel frame structures allowing for semi-rigid joint action. In *Steel Structures: Recent Research Advances and their Application to Design*, ed. M. N. Pavlovic. Elsevier Applied Science, London, 1986, pp. 136-82.
 23. Poggi, C., A finite element model for the analysis of flexibly connected steel frames. *International Journal for Numerical Methods in Engineering*, 26 (1988) 2239-54.
 24. Popov, E.P., and Bertero, P., (1973), "Cyclic Loading of Steel Beams and Connections." *Journal Structural, ASCE*, Vol. 99, No. ST6, pp. 1189-1204.
 25. Rathbun, J. C., Elastic properties of riveted connection. *Transactions, ASCE*, 101 (1936) 524-63.
 26. Rodrigues, F. C., Saldanha A. C. & Pfeil M. S., Non-linear analysis of steel frames with semi-rigid connections, *Journal of Constructional Steel Research*, v 46, n 1-3, 1998, p 94-97
 27. Suko, M. & Adams, P. F., Dynamic analysis of multibay multistory frames. *Journal of the Structural Division, ASCE*, 97 (ST10) (October 1971) 2519-33.
 28. Tsai, K. C., Wu, S. W., and Popov, E. G., (1995), "Experimental Performance of Seismic Steel Beam-Column Moment Joints." *Journal of Structural Engineering*, Vol. 121, No.6, PP 925 931.